ENGINEERING TRANSACTIONS • *Engng. Trans.* • **51**, 4, 461–491, 2003
Polish Academy of Sciences • Institute of Fundamental Technological Research
10.24423/engtrans.483.2003

DEFORMATION ZONES IN GRANULAR MATERIALS IN HOPPERS DURING FILLING AND EMPTYING PROCESSES

Z. Mróz[1] I. Sielamowicz[2]

[1]**Institute of Fundamental Technological Research, PAS, Warsaw, Poland**
e-mail: zmroz@ippt.gov.pl

[2]**Białystok Technical University, Department of Civil Engineering, Białystok, Poland**
e-mail: sieliren@pb.bialystok.pl

The present paper is concerned with the simplified analysis of deformation and stress states in converging hoppers during filling and discharge of a granular material. The equilibrium conditions and stress-strain relations are satisfied for cylindrical slice elements assuming dependence of displacement and stress on radial coordinate. The elastic or elasto-plastic material model is used with the Coulomb yield condition and non-associated flow rule. The paper presents a detailed analysis of pressure evolution of a granular material on a hopper wall during the emptying process when the initial active state of pressure is transformed into the passive state. The growth of wall pressure associated with this process is demonstrated. The analytical treatment presented in this paper can be compared with the respective finite element solution.

1. Introduction

The processes of granular material filling, discharge and storage in silos are associated with numerous important problems, such as evolution of pressures on silo walls, modes of flow during filling and discharge of material, particle segregation, effect of vibration and aeration, etc. The theoretical treatments of such problems are usually based on simplified material models, treating the granular material as linear elastic satisfying Hooke's law or perfectly plastic satisfying Coulomb yield condition and the associated or non-associated flow rule. A more realistic material model is based on the assumption of density hardening, with the varying cohesion dependent on the material density. Also the simplified geometry of silo was assumed in theoretical analysis, by considering plane converging or conical hoppers. The numerical treatment of granular

flow problems using the finite element method can also be found in the literature [1–4]. A large group of papers related to flow in converging channels is based on the assumption of radial flow velocity and steady or transient state of flow [5–11]. By accounting for gravity and inertial forces, the rate of discharge of material can be determined [12] assuming a rigid, perfectly plastic material model. Similarly, the stress state and material pressure on hopper walls can be determined [5, 6, 13–15]. The density hardening model introduced by Jenike [14–15] provided the possibility to predict the required outlet area for continuing flow and to characterize more realistically the important material parameters, in particular, the varying cohesion with material density and critical state parameters.

The present paper is devoted to the simplified analysis of material stress evolution during the filling and emptying processes in converging channels. To provide analytical treatment the simplifying assumptions are made, similarly as in other analyses [16, 17]. First, the simplified radial velocity and displacement fields are assumed, so the stress field depends only on the radial coordinate and the material–wall interaction is treated by introducing tractions at the interface into the equilibrium conditions. The elastic and elasto-plastic material model is assumed satisfying the Coulomb yield condition and the non-associated flow rule satisfying the incompressibility condition. With these assumptions the state of material after filling and the transient states during emptying are analysed in detail. It is shown that the initial stress state after filling is varying essentially passing from the so called "active pressure state" to the "passive pressure state", with the transition of the major principal stress in the radial direction to the major stress in circumferential direction during the emptying process. The transition from the filling stage to the emptying stage is achieved by assuming the variation of boundary conditions at the bottom boundary, namely from vanishing radial displacement to imposed displacement, usually dependent on controlled emptying procedure. The analysis, though based on simplified assumptions, allows for specifying the stress and wall pressure evolution in function of material parameters of the granular material. This analysis may prove important in assessment of pressure growth during emptying and also for comparison with numerical solutions obtained for a discretized problem by finite elements. The numerical elastic analysis of stress distribution after thr filling process using the finite element method was presented by OOI and ROTTER [2]. The stress distribution similar to that predicted in the present paper was obtained and the plastic zone was exhibited in the upper portion of the hopper. However, so far, there was no treatment in the literature of the transient stress evolution during the emptying process. A more detailed analysis and extensive discussion can be found in the research report by CZ. SZYMAŃSKI and Z. MRÓZ [18].

2. Fundamental equations of the problem

2.1. Constitutive equations

The constitutive relations and equilibrium or strain-displacement equations will be formulated in the Cartesian x_1, x_2, x_3, cylindrical (r, θ) or spherical r, θ, φ coordinates. The small strain theory is used with the usual linear relations between strain and displacements. The compressive stresses and contractive strains are assumed as positive, as is usually assumed in soil mechanics. The stress and strain tensors are decomposed into deviatoric and spherical parts, thus

$$\sigma_{ij} = s_{ij} + p\delta_{ij}, \qquad \varepsilon_{ij} = e_{ij} + \frac{1}{3}\varepsilon_\nu \delta_{ij}, \tag{2.1}$$

where $p = \frac{1}{3}\sigma_{kk}$ and $\varepsilon_\nu = \varepsilon_{kk}$ and δ_{ij} is the Kronecker delta.

Consider an elastic-perfectly, plastic model of the material (Fig. 1). Here we neglect the effect of density hardening and softening and critical state regime, typical for granular materials and powders.

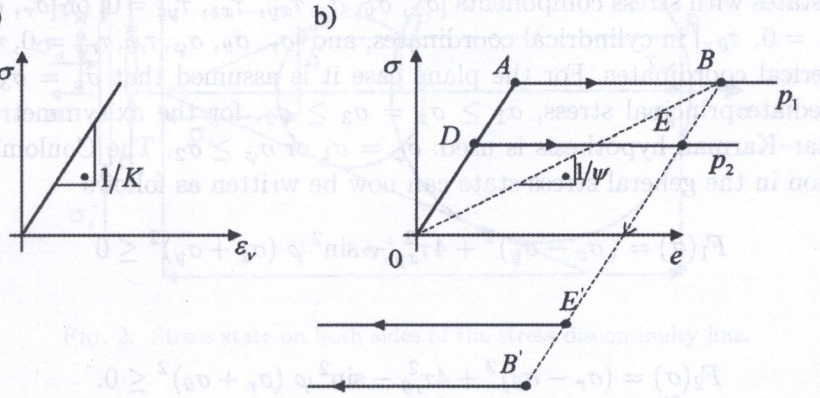

FIG. 1. Linear elastic a) and elastoplastic b) material model.

In the elastic state, the Hooke's law applies, so we have for an isotropic material

$$\varepsilon_{ij} = K\sigma\delta_{ij} + \frac{1}{2G}s_{ij}, \qquad i,j = 1,2,3, \tag{2.2}$$

where K is the bulk compliance modulus and G is the shear stiffness modulus of the material. We have also the familiar relations

$$K = \frac{1-2\nu}{E}, \qquad G = \frac{E}{2(1+\nu)}, \tag{2.3}$$

where E and ν are the Young modulus and Poisson ratio.

In the plastic regime, the Coulomb yield condition for a cohesionless material is assumed to be valid, thus

$$f(\underset{\sim}{\sigma}) = (\sigma_1 - \sigma_2) - (\sigma_1 + \sigma_3)\sin\varphi \leq 0, \tag{2.4}$$

where $\sigma_1 \geq \sigma_2 \geq \sigma_3 > 0$ are the principal stresses, and φ denotes the friction angle which is assumed as constant. The deformation theory is applied, so the finite stress–strain relations can be assumed in the elasto–plastic regime

$$\varepsilon_{ij} = K\sigma\delta_{ij} + \psi s_{ij}, \tag{2.5}$$

where $\psi > 0$ a secant compliance modulus dependent on the plastic strain value. In the elastic regime $\psi = \dfrac{1}{2G}$ and in the plastic regime $\psi = \|\underset{\sim}{e}\| / \|\underset{\sim}{s}\|$, where $\|\underset{\sim}{e}\| = (e_{ij}e_{ij})^{1/2}$ and $\|\underset{\sim}{s}\| = (s_{ij}s_{ij})^{1/2}$ are the moduli of strain and stress deviators.

The analysis will be performed for plane strain or axisymmetric stress and strain states with stress components $[\sigma_x, \sigma_y, \sigma_z, \tau_{xy}, \tau_{xz}, \tau_{yz} = 0]$ or $[\sigma_r, \sigma_\theta, \sigma_z, \tau_{r\theta}, \tau_{rz} = 0, \tau_{\theta z}]$ in cylindrical coordinates, and $[\sigma_r, \sigma_\theta, \sigma_\varphi, \tau_{r\theta}, \tau_{r\varphi} = 0, \tau_{\theta\varphi} = 0]$ in spherical coordinates. For the plane case it is assumed that $\sigma_z = \sigma_3$ is the intermediate principal stress, $\sigma_1 \geq \sigma_z = \sigma_3 \geq \sigma_2$, for the axisymmetric case the Haar–Karman hypothesis is used: $\sigma_\varphi = \sigma_1$ or $\sigma_\varphi \geq \sigma_2$. The Coulomb yield condition in the general stress state can now be written as follows

$$F_1(\underset{\sim}{\sigma}) = (\sigma_x - \sigma_y)^2 + 4\tau_{xy}^2 - \sin^2\varphi\,(\sigma_x + \sigma_y)^2 \leq 0 \tag{2.6}$$

or

$$F_2(\underset{\sim}{\sigma}) = (\sigma_r - \sigma_\theta)^2 + 4\tau_{r\theta}^2 - \sin^2\varphi\,(\sigma_r + \sigma_\theta)^2 \leq 0. \tag{2.7}$$

Consider a physical plane or surface Π with the unit normal and tangent vectors $\underline{n}$ and $\underline{t}$. Asssume that the traction is specified on Π, so the stress components σ_n, τ_{nt} are given. From the yield condition written in the local reference system n, t

$$F_3(\underset{\sim}{\sigma}) = (\sigma_n - \sigma_t)^2 + 4\tau_{nt}^2 - \sin^2\varphi\,(\sigma_n + \sigma_t)^2 \leq 0 \tag{2.8}$$

the value of σ_t can be specified provided $|\tau_{nt}| < \sigma_n \operatorname{tg}\varphi$. There are two solutions for σ_t in the plastic state, namely

$$\sigma_t = \frac{(1 + \sin^2\varphi)\,\sigma_n \mp 2\sqrt{\sigma_n^2 \sin^2\varphi - \tau_{nt}^2\cos^2\varphi}}{\cos^2\varphi}, \tag{2.9}$$

where $\sigma_t^{(+)}$ is the maximal state and $\sigma_t^{(-)}$ the minimal state. They are illustrated by Mohr circle in Fig. 2. In this figure the stress pole position is at P and two stress circles tangent to the Coulomb envelope specify the stress state at the surface Π. If the stress circles are not tangent, the elastic or rigid state occurs at the surface Π. If Π separates two material domains and is the interface separating maximal and minimal plastic state or both sides, then it is the stress discontinuity surface. The components σ_n and τ_{nt} are continuous on Π, but σ_t suffers discontinuity, so we have

$$[\sigma_n] = 0\,, \quad [\tau_{nt}] = 0, \quad [\sigma_t] = \frac{4\sqrt{\sigma_n^2 \sin^2\varphi - \tau_{nt}^2 \cos^2\varphi}}{\cos^2\varphi}, \tag{2.10}$$

where [] denotes the discontinuity of the enclosed symbols.

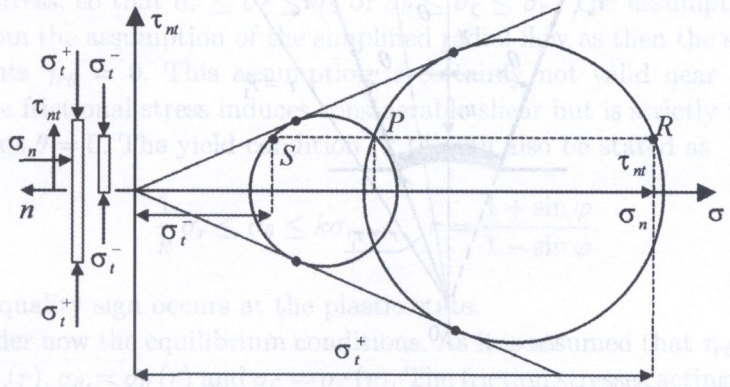

FIG. 2. Stress state on both sides of the stress discontinuity line.

When considering pressure of granular material on silo walls, we distinguish passive and active regimes. For passive regime the normal pressure σ_n is greater than σ_t (minimal state) and for active regime σ_n is smaller than σ_t. In fact, the active pressure on the wall is usually several times smaller than the pressure in passive regime. The active states are usually generated during filling the hopper and passive states develop during emptying. However, there is a transient state when the emptying process starts and the upper part of the hopper is still in active state with the passive regime progressing towards the upper boundary. This transient state is most dangerous to the structure containing the granular material as the travelling pressure peak develops at the interface Π between active and passive regimes and moves towards the upper boundary.

The present analysis is aimed at specifcation of this pressure evolution during the transient state. For a rigid-plastic material, the interface Π constitutes the

stress discontinuity surface and the effect of pressure peak can be easily traced. The present paper provides the analysis for an elastio-plastic material for which there is no stress discountinuity. The treatment for a rigid-plastic material involving stress discountinuity interface will be presented in a separate paper.

2.2. *Static and kinematic equations*

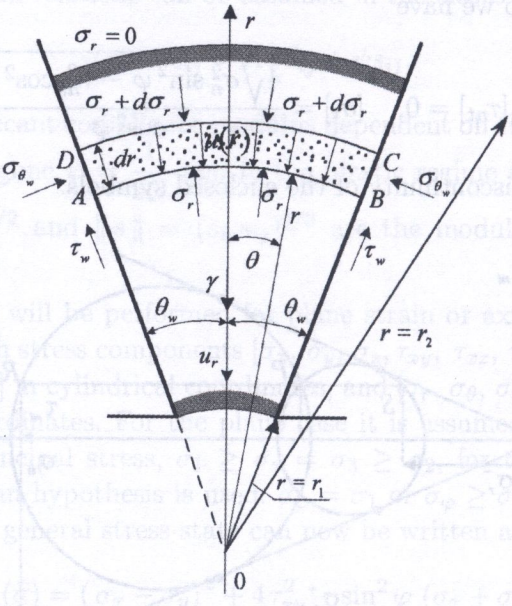

FIG. 3. Simplified radial flow in the hopper: stresses acting on the element ABCD.

Referring to Fig. 3 consider a plane wedge-shaped or conical hopper and select the sign θ of cylindrical r or spherical coordinate systems r, θ, z and r, θ, φ. In the plane case the z-axis is orthogonal to the plane r, θ of flow and in the conical hopper case, the plane r, θ lies in one of meridional planes specified by the angle $\varphi = \text{const}$. The simplified radial displacement field depending only on r is assumed in both cases and it can be expressed as follows

$$u_r = -u(r), \qquad u_\theta = 0, \qquad u_\zeta = 0, \tag{2.11}$$

where $\zeta = z$ for the wedge shaped hopper and $\zeta = \varphi$ for the conical hopper. In the following, it will be assumed that $\zeta = (1-m)z + m\varphi$, where $m = 0$ for the wedge hopper and $m = 1$ for the conical hopper [6]. The strain components in both cases now are

$$\varepsilon_r = -\frac{du_r}{dr} = \frac{du}{dr}, \qquad \varepsilon_\theta = -\frac{u_r}{r} = \frac{u}{r}, \qquad \varepsilon_\zeta = -\frac{mu_r}{r} = m\frac{u}{r}, \tag{2.12}$$

(2.12) [cont.)
$$\gamma_{r\theta} = 0, \qquad \gamma_{\theta\zeta} = 0, \qquad \gamma_{\zeta r} = 0.$$

The constitutive relations for the elasto–plastic regime can now be written as follows

(2.13)
$$\varepsilon_r = K\sigma + \psi\, s_r, \qquad \varepsilon_\theta = K\sigma + \psi\, s_\theta, \qquad \varepsilon_\zeta = K\sigma + \psi\, s_\zeta,$$
$$\gamma_{r\theta} = \gamma_{\theta\zeta} = \gamma_{\zeta r} = 0$$

and for the elastic case there is $\psi = \dfrac{1}{2G}$. The yield condition now is

(2.14)
$$F(\sigma) = (\sigma_r - \sigma_\theta)^2 - \sin^2\varphi\,(\sigma_r + \sigma_\theta)^2 \leq 0$$

since σ_r, σ_θ and σ_ζ are assumed as principal stresses with σ_ζ being the intermediate stress, so that $\sigma_r \leq \sigma_\zeta \leq \sigma_\theta$ or $\sigma_\theta \leq \sigma_\zeta \leq \sigma_r$. The assumption $\tau_{r\theta} = 0$ results from the assumption of the simplified radial flow as then the shear strain components $\gamma_{r\theta} = 0$. This assumption is certainly not valid near the hopper wall where frictional stress induces considerable shear but is strictly valid at the hopper axis $\theta = 0$. The yield condition (2.14) can also be stated as

(2.15)
$$\frac{1}{k}\sigma_r \leq \sigma_\theta \leq k\sigma_r, \qquad k = \frac{1+\sin\varphi}{1-\sin\varphi}$$

and the equality sign occurs at the plastic state.

Consider now the equilibrium conditions. As it is assumed that $\tau_{r\theta} = 0$, there is $\sigma_r = \sigma_r(r)$, $\sigma_\theta = \sigma_\theta(r)$ and $\sigma_\zeta = \sigma_\zeta(r)$. The friction stresses acting at the wall will be treated as the reaction stresses not entering the constitutive equations. These friction stresses satisfy the Coulomb friction condition

(2.16)
$$\tau_{r\theta}|_{\theta=\theta_w} = \tau_w = \sigma_\theta|_{\theta=\theta_w}\,\mathrm{tg}\mu, \qquad \mu = \text{const.}$$

Consider the equilibrium of an element ABCD shown in Fig. 3, bounded by the circular segments r and $r+dr$ and the radial lines $\theta = \mp\theta_w$. Accounting for shear stresses at the wall and the specific gravity forces $\gamma = \gamma(r)$, the equilibrium equation takes the form for the wedge hopper

(2.17)
$$\frac{d}{dr}(r\sigma_r) - \frac{\tau_w\cos\theta_w + \sigma_{\theta w}\sin\theta_w}{\sin\theta_w} + \gamma\frac{r\theta_w}{\sin\theta_w} = 0$$

and for the conical hopper we have

(2.18)
$$\frac{d}{dr}(r^2\sigma_r) - 2r\frac{\tau_w\cos\theta_w + \sigma_{\theta w}\sin\theta_w}{\sin\theta_w} + \gamma\frac{2r^2}{1+\cos\theta_w} = 0.$$

These two equations can now be written as

$$\frac{d\sigma_r}{dr} - \frac{(m+1)\,(\alpha\sigma_\theta - \sigma_r)}{r} + \gamma_m \gamma = 0, \tag{2.19}$$

where

$$\alpha = 1 + \mathrm{tg}\mu\,\mathrm{ctg}\theta_w, \qquad \gamma_m = (m+1)\left[(1-m)\frac{\theta_w}{\sin\theta_w} + \frac{m}{1+\cos\theta_w}\right] \tag{2.20}$$

and $m = 0$ for the wedge hopper, $m = 1$ for the conical hopper.

From the strain–displacement relations (2.12) it follows that the compatibility conditions take the form

$$\frac{d}{d_r}(r\varepsilon_\theta) - \varepsilon_r = 0, \qquad \varepsilon_\zeta = m\varepsilon_\theta, \qquad m = 0, 1. \tag{2.21}$$

Using the constitutive equations (2.13), the stress components can be substituted to (2.21), so we obtain

$$\frac{d}{dr}\left[(K-\psi)\,\sigma + \psi\,\sigma_\theta\right] + \frac{1}{r}\psi\,(\sigma_\theta - \sigma_r) = 0, \tag{2.22}$$

$$(K-\psi)\sigma + \psi\sigma_\zeta = m\left[(K-\psi)\,\sigma + \psi\sigma_\theta\right] = 0.$$

The pressure σ and the stress σ_ζ can be expressed in terms of σ_r, σ_θ and ψ, thus

$$\sigma = \frac{\psi\left[\sigma_r + (m+1)\,\sigma_\theta\right]}{(m+2)\,\psi + (1-m)\,K},$$

$$\sigma_\zeta = \frac{(\psi - K)\,(1-m)\,\sigma_r + \left[\psi\,(1+2m) - K\,(1-m)\right]\sigma_\theta}{(m+2)\,\psi + (1-m)\,K} \tag{2.23}$$

and the first equation (2.22) can be written as

$$\frac{d}{dr}\left[\psi\frac{(K-\psi)\,\sigma_r + (\psi+2K)\,\sigma_\theta}{(m+2)\,\psi + (1-m)\,K}\right] + \frac{1}{r}\psi\,(\sigma_\theta - \sigma_r) = 0. \tag{2.24}$$

The constitutive equations are based on the assumption that plastic strain is incompressible, so there is no significant density variation of the material, so it is assumed that $\gamma = \mathrm{const}$ during the filling and emptying processes. This is in fact physically not accurate assumption since the material undergoes compaction during filling and exhibits dilatancy during emptying.

The displacement field can be expressed in terms of stress components by using the constitutive equations, then in view of (2.23) there is

$$u = r\varepsilon_\theta = r\,(K\sigma + \psi s_\theta) = r\left[(K-\psi)\,\sigma + \psi\sigma_\theta\right] \tag{2.25}$$

$$= r\psi\frac{(K-\psi)\,\sigma_r + (\psi+2K)\,\sigma_\theta}{(m+2)\,\psi + (1-m)\,K}.$$

Let us now discuss the boundary conditions. It is assumed the upper surface $r = r_2$ is free, so the radial stress vanishes

$$\sigma_r(r_2) = 0. \tag{2.26}$$

The bottom surface $r = r_1$ is rigidly supported during the filling process, but during the emptying process the displacement is induced, thus controlling the intensity of discharge, so we have

$$\begin{aligned} u(r_1) &= 0 \quad - \text{filling stage}, \\ u(r_1) &= u_1 \quad - \text{discharge stage}. \end{aligned} \tag{2.27}$$

The bottom surface $r = r_1$ is assumed as fixed during both stages.

At the hopper walls for $\theta = \mp\theta_w$ the friction stresses are acting $\tau_w = \sigma_\theta(r)\mathrm{tg}\mu$, but they are included in the equilibrium equations, so there are no boundary conditions stated for $\theta = \mp\theta_w$. In fact, the simplified radial flow satisfies the kinematic constraints of the walls.

As there exist elastic and plastic zones within the hopper, the usual continuity conditions are specified at the interfaces

$$r = \eta, \qquad [\sigma_r] = 0, \qquad [u_r] = 0. \tag{2.28}$$

2.3. Non-dimensional form of equations

Introducing the non-dimensional variables $\overline{r} = \dfrac{r}{r_1}$, $\overline{\eta} = \dfrac{\eta}{r_1}$ the stress and displacement components can be reduced to a non-dimensional form

$$\begin{aligned} &\overline{\sigma}_r = \frac{\sigma_r}{\gamma\, r_1}, \qquad \overline{\sigma}_\theta = \frac{\sigma_\theta}{\gamma\, r_1}, \qquad \overline{\sigma}_\varsigma = \frac{\sigma_\varsigma}{\gamma\, r_1}, \\ &\overline{\tau}_w = \frac{\tau_w}{\gamma\, r_1}, \qquad \overline{u} = \frac{E\, u}{\gamma\, r_1^2}, \qquad \overline{\psi} = 2\,G\psi = \frac{E}{1+\nu}\psi \end{aligned} \tag{2.29}$$

and the fundamental equations (2.16), (2.19)–(2.25) now are

$$\begin{aligned} &\frac{d\,\overline{\sigma}_r}{d\,\overline{r}} - \frac{(m+1)\,\alpha\overline{\sigma}_\theta - \overline{\sigma}_r}{\overline{r}} + \gamma_m = 0, \\ &\frac{d}{d\overline{r}}\left[\frac{\overline{\psi}(\overline{\sigma}_\theta - \overline{\sigma}_r) + \nu_1(2\overline{\sigma}_\theta + \overline{\sigma}_r)}{\overline{\psi}\,(m+2) + \nu_1\,(1-m)}\overline{\psi}\right] + \frac{1}{\overline{r}}\overline{\psi}\,(\overline{\sigma}_\theta - \overline{\sigma_r}) = 0, \end{aligned} \tag{2.30}$$

$$\overline{\sigma}_\varsigma = \frac{(\overline{\psi}-\nu_1)(1-m)\,\overline{\sigma}_r + [\overline{\psi}(1+2m)-\nu_1(1-m)]\,\overline{\sigma}_\theta}{\overline{\psi}(m+2)+\nu_1(1-m)},$$

(2.30) [cont.]
$$\overline{\tau}_w = \overline{\sigma}_\theta \operatorname{tg}\mu,$$

$$\overline{u} = \overline{r}(1+\nu)\,\overline{\psi}\frac{\overline{\psi}(\overline{\sigma}_\theta - \overline{\sigma}_r) + \nu_1(2\overline{\sigma}_\theta + \overline{\sigma}_r)}{\overline{\psi}(m+2)+\nu_1(1-m)}.$$

For the elastic region we have $\overline{\psi} = 1$ and $\overline{\psi} \geq 1$ for the elasto-plastic state. Further, the following symbols are used

$$\alpha = 1 + \operatorname{tg}\mu\ \operatorname{ctg}\theta_w, \quad k = \frac{1+\sin\varphi}{1-\sin\varphi}, \qquad \nu_1 = \frac{1-2\nu}{1+\nu},$$

(2.31)
$$\gamma_m = (m+1)\left[(1-m)\frac{\theta_w}{\sin\theta_w} + \frac{m}{1+\cos\theta_w}\right].$$

3. Solutions in elastic and elasto–plastic regions

3.1. Elastic solution

Let us first discuss the elastic solution. Setting $\overline{\psi} = 1$ in $(2.30)_{1,2}$ we have

$$\frac{d\sigma_r}{dr} - \frac{(m+1)(\alpha\sigma_\theta - \sigma_r)}{r} + \gamma_m = 0, \quad m = 0,\ 1,$$

(3.1)
$$\frac{d}{dr}\left[\frac{(\sigma_\theta - \sigma_r) + \nu_1(2\sigma_\theta + \sigma_r)}{(m+2)+\nu_1(1-m)}\right] + \frac{1}{r}(\sigma_\theta - \sigma_r) = 0.$$

The non-dimensional quantities will be used in the subsequent analysis and the dash over the symbol is omitted. The set (3.1) can be rewritten as follows

$$\frac{d\sigma_r}{dr} + \frac{m+1}{r}\sigma_r - \frac{(m+1)\,\alpha}{r}\sigma_\theta + \gamma_m = 0,$$

(3.2)
$$\frac{d\sigma_\theta}{dr} - \frac{1}{r}\sigma_r + \frac{(m\nu+1) - \alpha(m+1)\,\nu}{(1-\nu)\,r}\sigma_\theta + \frac{\nu}{1-\nu}\gamma_m = 0$$

and the general integrals have the form

$$\sigma_r^e = A_m r^{\lambda_{1m}} + B_m r^{\lambda_{2m}} - l_m \gamma_m r,$$

(3.3)
$$\sigma_\theta^e = \frac{\lambda_{1m} + (m+1)}{\alpha(m+1)} A_m r^{\lambda_{1m}} + \frac{\lambda_{2m} + (m+1)}{\alpha(m+1)} B_m r^{\lambda_{2m}} - d_m \gamma_m r,$$

where A_m, B_m are the integration constants and the remaining symbols are defined as follows

$$\lambda_{1m} = \frac{1}{2}\left(a_m + \sqrt{\Delta_m}\right), \qquad \lambda_{2m} = \frac{1}{2}\left(a_m - \sqrt{\Delta_m}\right),$$

$$a_m = \frac{\alpha(m+1)\nu - (m+2-\nu)}{1-\nu},$$

$$b_m = \frac{(m+1)(m\nu+1)(\alpha-1)}{1-\nu}, \qquad \Delta_m = a_m^2 + 4b_m,$$

$$l_m = \frac{2+\nu(m-1)}{(m+2)\left[(m-1)\nu+2\right] - \alpha(m+1)\left[(m+1)\nu+1\right]}, \tag{3.4}$$

$$d_m = \frac{1+\nu(m+1)}{(m+2)\left[(m-1)\nu+2\right] - \alpha(m+1)\left[(m+1)\nu+1\right]},$$

$$\alpha = 1 + \operatorname{tg}\mu \operatorname{ctg}\theta_w,$$

$$\gamma_m = (m+1)\left[(1-m)\frac{\theta_w}{\sin\theta_w} + \frac{m}{1+\cos\theta_w}\right],$$

where $m = 0$ for the plane case and $m = 1$ for the axisymmetric case. Further, we have

$$\sigma_\zeta^e = \frac{(1-m)\nu\sigma_r^e + (m+\nu)\sigma_\theta^e}{m\nu+1}, \tag{3.5}$$

$$\tau_w^e = \sigma_\theta^e \operatorname{tg}\mu$$

and

$$u^e = \frac{(1+\nu)}{m\nu+1}\left(\beta_{1m} A_m r^{\lambda_{1m}} + \beta_{2m} B_m r^{\lambda_{2m}} + \chi_m \gamma_m r\right) r, \tag{3.6}$$

where

$$\beta_{1m} = \frac{(1-\nu)(\lambda_{1m}+m+1)}{\alpha(m+1)} - \nu, \quad \beta_{2m} = \frac{(1-\nu)(\lambda_{2m}+m+1)}{\alpha(m+1)} - \nu,$$

$$\chi_m = \frac{(2\nu-1)(m\nu+1)}{(m+2)\left[(m-1)\nu+2\right] - \alpha\,(m+1)\left[(m+1)\nu+1\right]}. \tag{3.7}$$

The solution presented is valid provided

$$\alpha \neq \alpha_m^{es} \equiv \frac{(m+2)\left[(m-1)\nu+2\right]}{(m+1)\left[(m+1)\nu+1\right]}, \quad m = 0,\ 1. \tag{3.8}$$

Let us note that when $\alpha = \alpha_m^{es}$, then l_m, d_m and λ_m tend to infinity.

For $\alpha = \alpha_m^{es}$, we have a different form of general integrals, called *a singular solution* specified by the relations

$$\sigma_r^{es} = A_m^s r + B_m^s r^{-a_m^s} - k_m \gamma_m^{es} r \ln r,$$

$$\sigma_\theta^{es} = \frac{m+2}{\alpha_m^{es}(m+1)} A_m^s r + \frac{(m+1)-a_m^s}{\alpha_m^{es}(m+1)} B_m^s r^{-a_m^s} - \frac{(m+2)\, k_m \gamma_m^{es}}{\alpha_m^{es}(m+1)} r \ln r + \frac{(1-k_m)\, \gamma_m^{es}}{\alpha_m^{es}(m+1)} r, \tag{3.9}$$

where A_m^s, B_m^s are the integration constants and

$$\alpha_m^{es} \equiv \frac{(m+2)\,[(m-1)\nu+2]}{(m+1)\,[(m+1)\nu+1]}, \qquad \theta_{w(m)}^{es} = \operatorname{arctg}\left(\frac{\operatorname{tg}\mu}{\alpha_m^{es}-1}\right),$$

$$\gamma_m^{es} = (m+1)\left[(1-m)\frac{\theta_{w(m)}^{es}}{\sin\theta_{w(m)}^{es}} + \frac{m}{1+\cos\theta_{w(m)}^{es}}\right],$$

$$a_m^s = \frac{(m+3)(m\nu+1)}{(m+1)\,\nu+1}, \tag{3.10}$$

$$k_m = \frac{[(m+1)\nu+1]\,[(m-1)\nu+2]}{(1-\nu)\,[(m^2+4m+1)\,\nu+(m+4)]}.$$

The displacement field for a singular solution is

$$u^{es} = \frac{(1+\nu)}{m\nu+1}\Big(\beta_{1m}^s A_m^s r + \beta_{2m}^s B_m^s r^{-\alpha_m^s} + \delta_m \gamma_m^{es} r - \varpi_m \gamma_m^{es} r \ln r\Big) r, \tag{3.11}$$

where

$$\beta_{1m}^s = \frac{(1-2\nu)(m\nu+1)}{(m-1)\nu+2}, \qquad \beta_{2m}^s = -\frac{(m+1)\,\nu+1}{m+2},$$

$$\delta_m = \frac{(1-2\nu)(m\nu+1)\,[(m+1)\,\nu+1]}{[(m^2+4m+1)\,\nu+m+4]\,[(m-1)\,\nu+2]}, \tag{3.12}$$

$$\varpi_m = \frac{(1-2\nu)(m\nu+1)\,[(m+1)\,\nu+1]}{(1-\nu)\,[(m^2+4m+1)\;\nu+m+4]}.$$

Consider now the filling and emptying processes for the elastic material. For the filling process the boundary conditions are

$$\sigma_r(r)\,\big|_{r=1/n} = 0, \qquad u(r)\Big|_{r=1} = 0, \qquad (n = r_1/r_2). \tag{3.13}$$

Using the general solutions (3.3) and (3.6) for stress and displacement fields, these conditions provide the equations for the constants A_m and B_m, namely

$$A_m \left(\frac{1}{n}\right)^{\lambda_{1m}} + B_m \left(\frac{1}{n}\right)^{\lambda_{2m}} - l_m \gamma_m \frac{1}{n} = 0,$$

(3.14)

$$\beta_{1m} A_m + \beta_{2m} B_m + \chi_m \gamma_m = 0,$$

and we have

$$A_m = \frac{\chi_m \gamma_m}{\beta_{1m}} (K_m - 1), \qquad B_m = -\frac{\chi_m \gamma_m}{\beta_{2m}} K_m,$$

(3.15)

where

$$K_m = \frac{1 + \dfrac{l_m}{\chi_m} \beta_{1m} n^{(\lambda_{1m}-1)}}{1 - \dfrac{\beta_{1m} n^{\lambda_{1m}-\lambda_{2m}}}{\beta_{2m}}}.$$

(3.16)

For the emptying process it is assumed that the upper surface is free, but the bottom material surface undergoes increasing displacement u_1 starting from the initial zero value. We assume therefore the boundary conditions

$$\sigma_r(r)|_{r=1/n} = 0, \qquad u(r)|_{r=1} = u_1, \qquad (n = r_1/r_2).$$

(3.17)

We obtain therefore the equations

$$A_m \left(\frac{1}{n}\right)^{\lambda_{1m}} + B_m \left(\frac{1}{n}\right)^{\lambda_{2m}} - l_m \gamma_m \frac{1}{n} = 0,$$

$$\frac{1+\nu}{m\nu+1}\left(\beta_{1m} A_m + \beta_{2m} B_m + \chi_m \gamma_m\right) = u_1,$$

(3.18)

and the integration constants A_m, B_m now depend on the emptying parameter u_1, thus

$$A_m(u_1) = \frac{q_m(u_1)}{\beta_{1m}}\left[1 - K_m(u_1)\right],$$

$$B_m(u_1) = \frac{q_m(u_1)}{\beta_{2m}} K_m(u_1),$$

(3.19)

where

$$q_m(u_1) = \frac{1+m\nu}{1+\nu} u_1 - \chi_m \gamma_m,$$

$$K_m(u_1) = \frac{1 - \dfrac{l_m \gamma_m}{q_m(u_1)} \beta_{1m} (n)^{(\lambda_{1m}-1)}}{1 - \dfrac{\beta_{1m}}{\beta_{2m}} n^{(\lambda_{1m}-\lambda_{2m})}}.$$

(3.20)

Similar relations are obtained for the singular case but the respective formulae are not quoted here.

The illustrative solutions are obtained for both plane and axisymmetrical hoppers assuming the following parameters $\nu = 1/3$, $\mu = 30°$, $r_2/r_1 = 1/n = 15$, $\theta_w = 15°$ $30°$ and $\theta_w = \theta_w^{es}$, $m = 0, 1$ where θ_w^{es} denotes the singular value of the wedge angle, namely $\theta_w^{es} = 21° 03'$ for the wedge hopper, $m = 0$, $\theta_w^{es} = 35° 49'$, for the conical hopper, $m = 1$.

Figures 4a, b, c, d present the solutions for wedge hoppers after the filling process for three values of the angle θ_w.

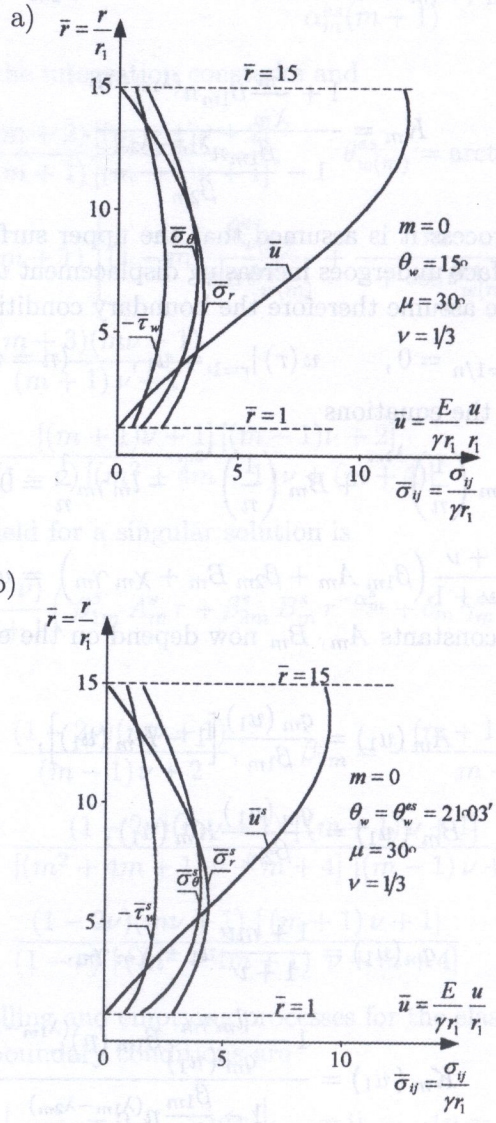

[FIG. 4 a, b]

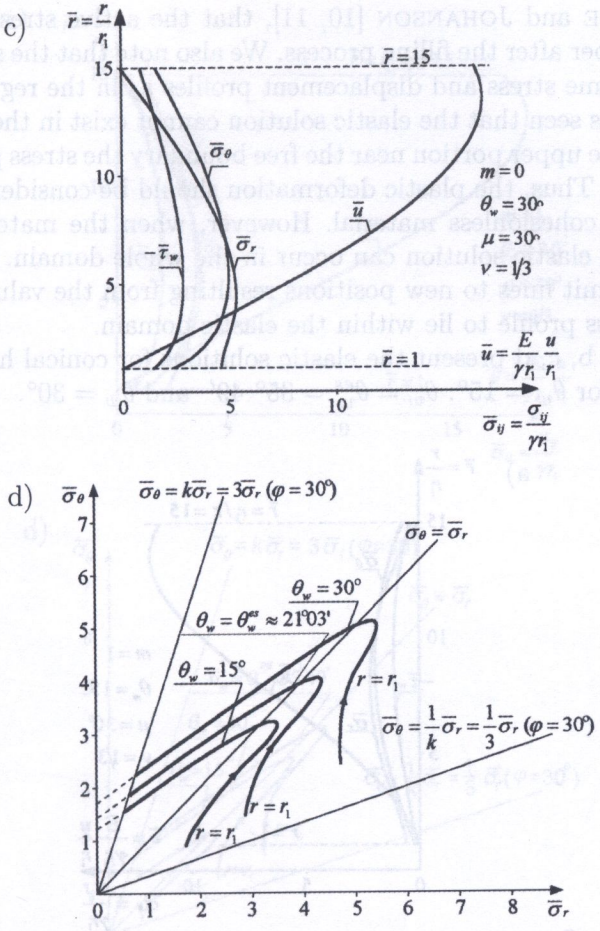

FIG. 4. Stress and displacement distribution in the wedge hopper after the filling process for three values of the hopper angle θ_w: a) $\theta_w = 15°$, b) $\theta_w^{es} = 21°03'$, c) $\theta_w = 30°$, d) stress profiles in the plane $\bar{\sigma}_r, \bar{\sigma}_\theta$.

The diagrams show the stress distributions $\sigma_r = \sigma_r(r)$, $\sigma_\theta = \sigma_\theta(r)$, $\sigma_\zeta = \sigma_\zeta(r)$ and $u = u(r)$ in the non-dimensional variables. The stress profile in the plane $\bar{\sigma}_r$, $\bar{\sigma}_\theta$ is shown in. Fig. 4d, where also the yield lines $\bar{\sigma}_\theta = \frac{1}{k}\bar{\sigma}_r$, and $\bar{\sigma}_\theta = k\bar{\sigma}_r$ are shown.

The following conclusions can be drawn from the elastic solutions for the filling process. It is seen that the maximal stress values occur in the middle part of the hopper. In the lower part the active stress state occurs, $\sigma_r^e > \sigma_\theta^e$, but in the upper part the passive state, $\sigma_r^e < \sigma_\theta^e$, develops. This character of stress distribution will change during the emptying process where the passive state will develop at the bottom hopper portion. This observation does not support the

view, of JENIKE and JOHANSON [10, 11], that the active stress state develops within the hopper after the filling process. We also note that the singular solution provides the same stress and displacement profiles as in the regular case.

Further, it is seen that the elastic solution cannot exist in the whole material domain as in the upper portion near the free boundary the stress path exceeds the elastic domain. Thus, the plastic deformation should be considered in the upper portion of the cohesionless material. However, when the material is cohesive, $c \neq 0$, then the elastic solution can occur in the whole domain. In fact, one can translate the limit lines to new positions resulting from the value of cohesion to assure the stress profile to lie within the elastic domain.

Figures 5 a, b, c, d present the elastic solutions for conical hoppers after the filling process for $\theta_w = 15°$, $\theta_w = \theta_w^{es} = 35°\ 49'$ and $\theta_w = 30°$.

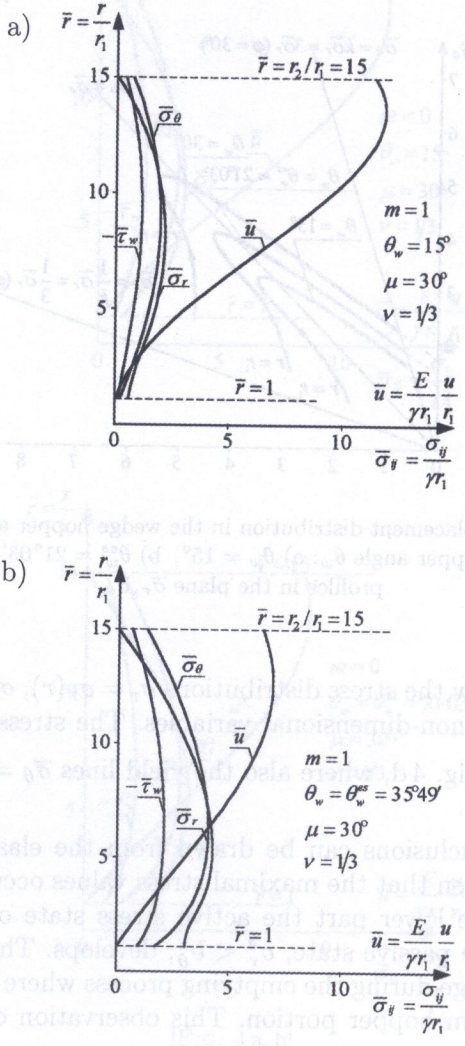

[FIG. 5 a, b]

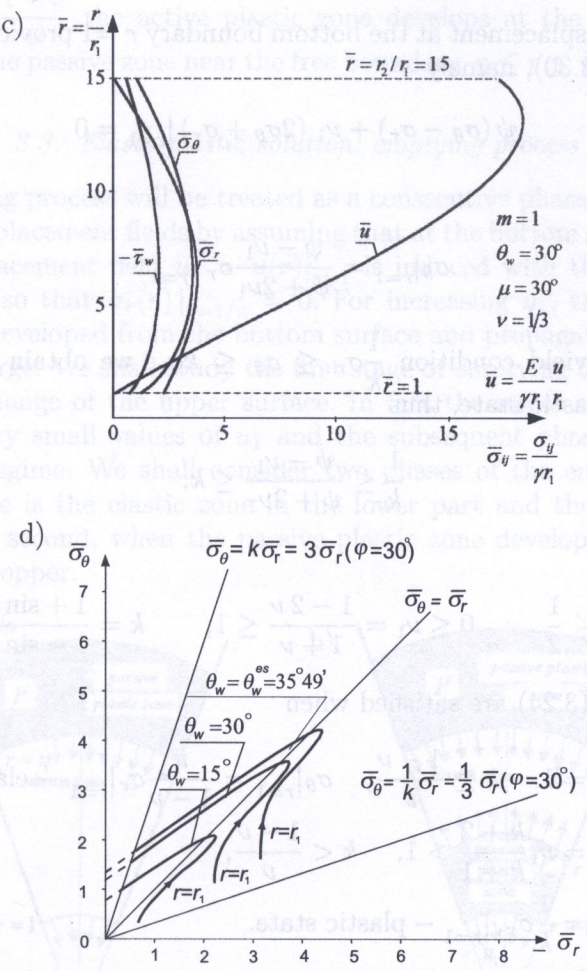

FIG. 5. Stress and displacement distributions after the filling process: a) $\theta_w = 15°$, b) $\theta_w = \theta_w^{es} = 35°\ 49'$, c) $\theta_w = 30°$, d) stress profiles in the plane $\bar{\sigma}_r$, $\bar{\sigma}_\theta$.

The same conclusions can be drawn as in the case of wedge hoppers, namely the existence of the plastic zone near the upper boundary and the combined active-passive stress function within the material.

3.2. Elasto-plastic solution

Let us now discuss the elasto-plastic solution assuming the perfectly-plastic material model. Depending on the value of material parameters there can be two different stress profiles. These profiles result from the boundary conditions

$$\sigma_r(r)|_{r=1/n} = 0, \qquad u(r)|_{r=1} = 0, \qquad (n = r_1/r_2). \tag{3.21}$$

The vanishing displacement at the bottom boundary $r=1$ provides the condition resulting from (2.30), namely

$$\psi(\sigma_\theta - \sigma_r) + \nu_1(2\sigma_\theta + \sigma_r)|_{r=1} = 0 \tag{3.22}$$

which provides

$$\sigma_\theta|_{r=1} = \frac{\psi - \nu_1}{\psi + 2\nu_1}\sigma_r|_{r=1}. \tag{3.23}$$

In view of the yield condition $\frac{1}{k}\sigma_r \leq \sigma_\theta \leq k\sigma_r$, we obtain the inequalities specifying the elastic state, thus

$$\frac{1}{k} \leq \frac{\psi - \nu_1}{\psi + 2\nu_1} \leq k. \tag{3.24}$$

Since

$$0 \leq \nu \leq \frac{1}{2}, \qquad 0 \leq \nu_1 = \frac{1-2\nu}{1+\nu} \leq 1, \qquad k = \frac{1+\sin\varphi}{1-\sin\varphi} \geq 1,$$

the inequalities (3.24) are satisfied when

$$\begin{aligned} &\psi|_{r-1} = 1, \quad k \geq \frac{1-\nu}{\nu}, \quad \sigma_\theta|_{r=1} = \frac{\nu}{1-\nu}\sigma_r|_{r=1} - \text{elastic state or,} \\ &\psi|_{r=1} = \nu_1\frac{k+2}{k+1} > 1, \quad k < \frac{1-\nu}{\nu}, \\ &\sigma_\theta|_{r=1} = \frac{1}{k}\sigma_r,|_{r=1} - \text{plastic state.} \end{aligned} \tag{3.25}$$

The expected stress profiles are shown in Fig. 6

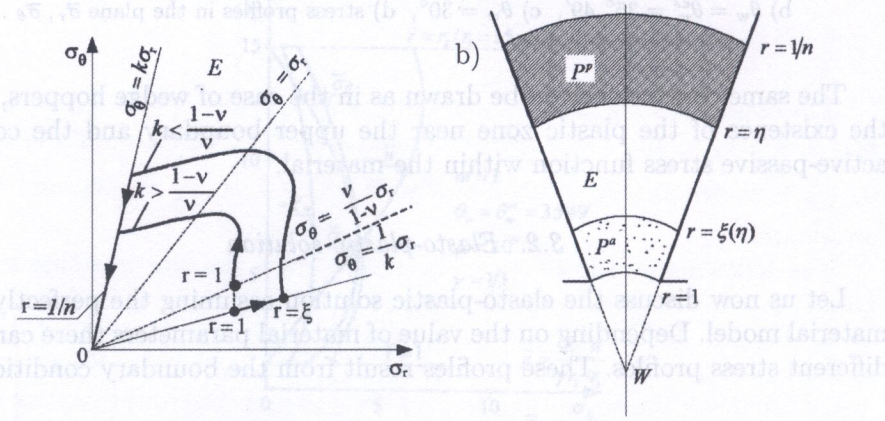

FIG. 6. Stress profiles for the elasto-plastic model: a) stress profiles in the plane σ_r, σ_θ, b) plastic and elastic zones within the hopper.

When $k > \dfrac{1-\nu}{\nu}$ the active plastic zone develops at the bottom domain $1 \le r \le \xi$ and the passive zone near the free boundary, $\eta \le r \le 1/n$, $(n = r_1/r_2)$.

3.3. Elasto-plastic solution: emptying process

The emptying process will be treated as a consecutive phase of the evolution of stress and displacement fields by assuming that at the bottom surface $r = 1$ the increasing displacement field $u_1 = u(r)|_{r=1}$ is induced with the upper surface remaining free, so that $\sigma_r(r)\,|_{r=1/n} = 0$. For increasing u_1, the passive stress regime will be developed from the bottom surface and propagate upward in the course of discharge. We shall study the first stage of emptying by neglecting the configuration change of the upper surface. In fact the stress evolution process develops for very small values of u_1 and the subsequent phase occurs within passive stress regime. We shall consider two phases of the emptying process: first, when there is the elastic zone in the lower part and the plastic zone in the upper part, second, when the passive plastic zone develops at the bottom domain of the hopper.

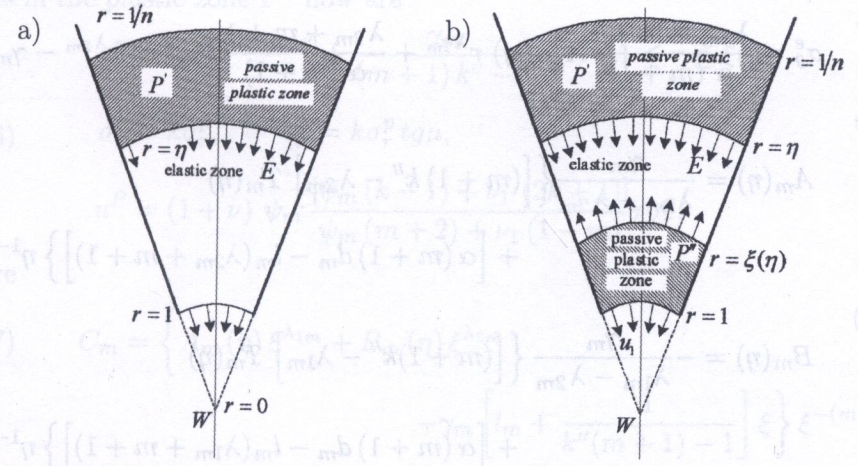

FIG. 7. Elastic and plastic zones in the a) initial and b) advanced stages of discharge.

3.3.1. Initial stage of emptying: elastic and plastic zone. Assume the boundary conditions as follows

$$\sigma_r(r)\,|_{r=1/n} = 0, \qquad u(r)\,|_{r=1} = -u_1 \qquad (n = r_1/r_2) \tag{3.26}$$

and the position of elasto-plastic interface $r = \eta$ depends on u_1, thus $\eta = \eta(u_1)$ or $u_1 = u_1(\eta)$. At the interface the stress and displacement continuity conditions are satisfied, thus

$$[\sigma_r] = [u] = 0, \quad \sigma_\theta = k\sigma_r, \quad \text{for} \quad r = \eta. \tag{3.27}$$

Taking the interface position $r = \eta$ as the process progression parameter, it is noted that for some value of $\eta(u_1) = \eta''$ the yield condition at the bottom surface is satisfied, so that

$$F_1(r, \eta(u_1))|_{r=1} = (k\sigma_r^e - \sigma_\theta^e)|_{r=1} = 0 \tag{3.28}$$

and for increasing values of u_1 or $\eta(u_1)$ the passive plastic zone starts to develop near the bottom surface.

Let us now discuss the details of the solution when the elastic and plastic zones E and P' exist within the solution domain. The plastic stress state within P' is specified by (3.22) and the elastic state within E is specified by (3.3). The integration constants $A_m(\eta)$, $B_m(\eta)$ are specified from the boundary condition at $r = 1/n$ and continuity conditions for $r = \eta$. We obtain within the zone P'.

$$\sigma_r^P = \gamma_m r T_m(r), \qquad T_m(r) = \frac{1 - (nr)^{(m+1)k''-1}}{(m+1)k'' - 1} \tag{3.29}$$

and within the zone E

$$\begin{aligned} \sigma_r^e &= A_m(\eta) r^{\lambda_{1m}} + B_m(\eta) r^{\lambda_{2m}} - \gamma_m l_m r, \\ \sigma_\theta^e &= \frac{\lambda_{1m} + m + 1}{\alpha(m+1)} A_m(\eta) r^{\lambda_{1m}} + \frac{\lambda_{2m} + m + 1}{\alpha(m+1)} B_m(\eta) r^{\lambda_{2m}} - \gamma_m d_m r, \end{aligned} \tag{3.30}$$

where

$$\begin{aligned} A_m(\eta) = \frac{\gamma_m}{\lambda_{1m} - \lambda_{2m}} \Big\{ \Big[(m+1)k'' - \lambda_{2m} \Big] T_m(\eta) \\ + \Big[\alpha(m+1) d_m - l_m(\lambda_{2m} + m + 1) \Big] \Big\} \eta^{1-\lambda_{1m}}, \end{aligned} \tag{3.31}$$

$$\begin{aligned} B_m(\eta) = -\frac{\gamma_m}{\lambda_{1m} - \lambda_{2m}} \Big\{ \Big[(m+1)k'' - \lambda_{1m} \Big] T_m(\eta) \\ + \Big[\alpha(m+1) d_m - l_m(\lambda_{1m} + m + 1) \Big] \Big\} \eta^{1-\lambda_{2m}}. \end{aligned}$$

The initiation of the emptying process starts for $u_1(\eta) = 0$ and proceeds for $u_1 > 0$. The value η' is specified from the condition (3.18), thus

$$\beta_{1m} A_m(\eta') + \beta_{2m} B_m(\eta') + \gamma_m \chi_m = 0. \tag{3.32}$$

The value η'' corresponds to the onset of plasticity at $r = 1$, specified by the condition

$$\begin{aligned} \frac{1}{\alpha(m+1)} \Big\{ \Big[(m+1)k'' - \lambda_{1m} \Big] A_m(\eta'') \\ + \Big[(m+1)k'' - \lambda_{2m} \Big] B_m(\eta'') \Big\} + \gamma_m (d_m - k l_m) = 0. \end{aligned} \tag{3.33}$$

Thus the emptying process with the elastic zone E in the lower domain occurs when $\eta' \le \eta \le \eta''$.

3.3.2. Advanced stage of emptying: solution with three zones P', E and P'' (Fig. 7b). The interface radius $r = \xi(\eta)$ between the elastic and plastic zones P'' in the bottom part of the hopper is specified from the yield condition

$$F_1 = k\sigma_r^e(r,\eta) - \sigma_\theta^e(r,\eta) = 0 \tag{3.34}$$

and there should be $1 \le \xi(\eta) \le \eta$. When $\xi = \eta$, both plastic zones P' and P'' contact each other and the whole material becomes plastic. The condition (3.34) provides the equation

$$F_1 = \frac{1}{\alpha(m+1)}\left\{\left[(m+1)k'' - \lambda_{1m}\right]A_m(\eta)\, r^{\lambda_{1m}} + \left[(m+1)k'' - \lambda_{2m}\right]B_m(\eta)\, r^{\lambda_{2m}}\right\} + \gamma_m(d_m - k\,l_m)\,r = 0, \tag{3.35}$$

where $A_m(\eta)$ and $B_m(\eta)$ are specified by (3.31). The stress and displacement states in the plastic zone P'' now are

$$\sigma_r^p = C_m r^{(m+1)k''} + \frac{\gamma_m}{(m+1)k'' - 1}r, \qquad 1 \le r \le \xi(\eta),$$

$$\sigma_\theta^p = k\sigma_r^p, \qquad \tau_w^p = k\sigma_r^p\, tg\mu, \tag{3.36}$$

$$u^P = (1+\nu)\,\psi_m \frac{[\psi_m(k-1) + \nu_1\,(2k+1)]}{\psi_m(m+2) + \nu_1(1-m)} r\sigma_r^p,$$

where

$$C_m = \left\{A_m(\eta)\,\xi^{\lambda_{1m}} + B_m(\eta)\,\xi^{\lambda_{2m}} - \gamma_m\left[l_m + \frac{1}{k''(m+1) - 1}\right]\xi\right\}\xi^{-(m+1)k''}, \tag{3.37}$$

$$k'' = \alpha k - 1.$$

The stress and displacement states in the elastic zone E are

$$\sigma_r^e = A_m(\eta)\, r^{\lambda_{1m}} + B_m(\eta)\, r^{\lambda_{2m}} - \gamma_m\, l_m r, \qquad \xi(\eta) \le r \le \eta,$$

$$\sigma_\theta^e = \frac{\lambda_{1m} + m + 1}{\alpha(m+1)}A_m(\eta)\, r^{\lambda_{1m}} + \frac{\lambda_{2m} + m + 1}{\alpha(m+1)}B_m(\eta)\, r^{\lambda_{2m}} - \gamma_m d_m r,$$

$$\sigma_\varsigma^e = \frac{(1-m)\,\nu\sigma_r^e + (m+\nu)\,\sigma_\theta^e}{m\nu + 1}, \qquad \tau_w = \sigma_\theta^e\, tg\mu, \tag{3.38}$$

$$u^e = \frac{(1+\nu)\,[(1-\nu)\,\sigma_\theta^e - \nu\sigma_r^e]}{m\nu + 1},$$

and in the upper plastic zone P' we have

$$\sigma_r^P = \gamma_m\, r\, T_m(r), \qquad \sigma_\theta^p = k\sigma_r^p, \qquad \tau_w^p = k\,\sigma_r^p\,\mathrm{tg}\mu,$$

$$\sigma_\xi^p = \frac{\psi_m\,[(1+2m)\,k+(1-m)] - \nu_1\,(1-m)\,(k+1)}{\psi_m\,(m+2)+\nu_1\,(1-m)}\sigma_r^p, \tag{3.39}$$

$$u^p = (1+\nu)\;\psi_m \frac{\psi_m\,(k-1)+\nu_1\,(2k+1)}{\psi_m\,(m+2)+\nu_1\,(1-m)} r\sigma_r^p, \qquad \eta \le r \le \frac{1}{n},$$

where

$$T_m(r) = \frac{1-(n\,r)^{(m+1)\,k''-1}}{(m+1)\,k''-1}, \qquad k'' = \alpha k - 1, \tag{3.40}$$

and $\psi_m(r,\eta)$ is the solution of the differential equation

$$\frac{d\psi_m}{dr} = \tag{3.41}$$

$$-\frac{\psi_m\,(\psi_m+\nu_1 m_1)\left\{\left[R'_m(r)+\dfrac{m+2}{r}\right](\psi_m+\nu_1 m_1)+\nu_1\left(k_1^P-m_1\right)R'_m(r)\right\}}{(\psi_m+\nu_1 m_1)^2+\nu_1^2\left(k_1^P-m_1\right)m_1},$$

where

$$R'_m(r) \equiv \frac{1}{\sigma_r^{p'}}\frac{d\sigma_r^{p'}}{dr} = \frac{1-(m+1)\,k''\,(n\,r)^{(m+1)k''-1}}{r\left[1-(n\,r)^{(m+1)k''-1}\right]}. \tag{3.42}$$

The solution of (3.40) is obtained numerically by applying the finite difference explicit integration scheme.

4. Illustrative numerical solutions.

Numerical solutions were generated for both plane and conical hoppers ($m=0$ and $m=1$), for two values of the hopper angle: $\theta_w = 15°$, $\theta_w = 30°$ and for three values of the position of the upper three surface: $n = r_1/r_2 = 5, 10, 15$. The numerical results are illustrated in Figs. 8–10 presenting stress and displacement distributions in consecutive stages of the discharge process.

Figures 8 a, b, c, d present the stress and displacement evolution during consecutive stages of emptying of the wedge hopper for $n = 1/5$, $\theta_w = 15°$, $\mu = 30°$, $\nu = 1/3$. As σ_θ represents also the wall pressure evolution, it is seen that when the plastic passive zone P'' propagates upward the wall pressure reaches its maximum at the instantaneous interface position $r = \xi$ between P'' and E. There

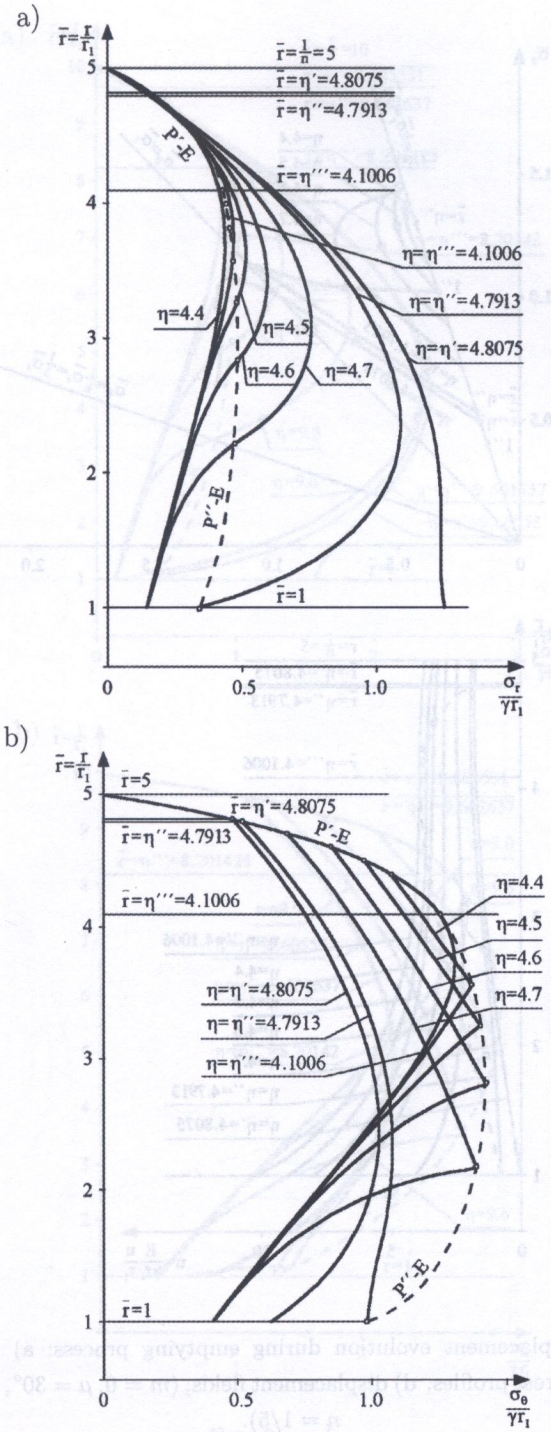
a)
$\bar{r}=\frac{r}{r_1}$
$\bar{r}=\frac{1}{n}=5$
$\bar{r}=\eta'=4.8075$
$\bar{r}=\eta''=4.7913$
P'-E
$\bar{r}=\eta'''=4.1006$
$\eta=\eta'''=4.1006$
$\eta=\eta''=4.7913$
$\eta=\eta'=4.8075$
η=4.4
η=4.5
η=4.6
η=4.7
P''-E
$\bar{r}$=1
5
4
3
2
1
0
0.5
1.0
$\frac{\sigma_r}{\gamma r_1}$
b)
$\bar{r}=\frac{r}{r_1}$
$\bar{r}$=5
$\bar{r}=\eta'=4.8075$
$\bar{r}=\eta''=4.7913$
P'-E
$\bar{r}=\eta'''=4.1006$
η=4.4
η=4.5
η=4.6
η=4.7
$\eta=\eta'=4.8075$
$\eta=\eta''=4.7913$
$\eta=\eta'''=4.1006$
P''-E
$\bar{r}$=1
5
4
3
2
1
0
0.5
1.0
$\frac{\sigma_\theta}{\gamma r_1}$

FIG. 8. a, b

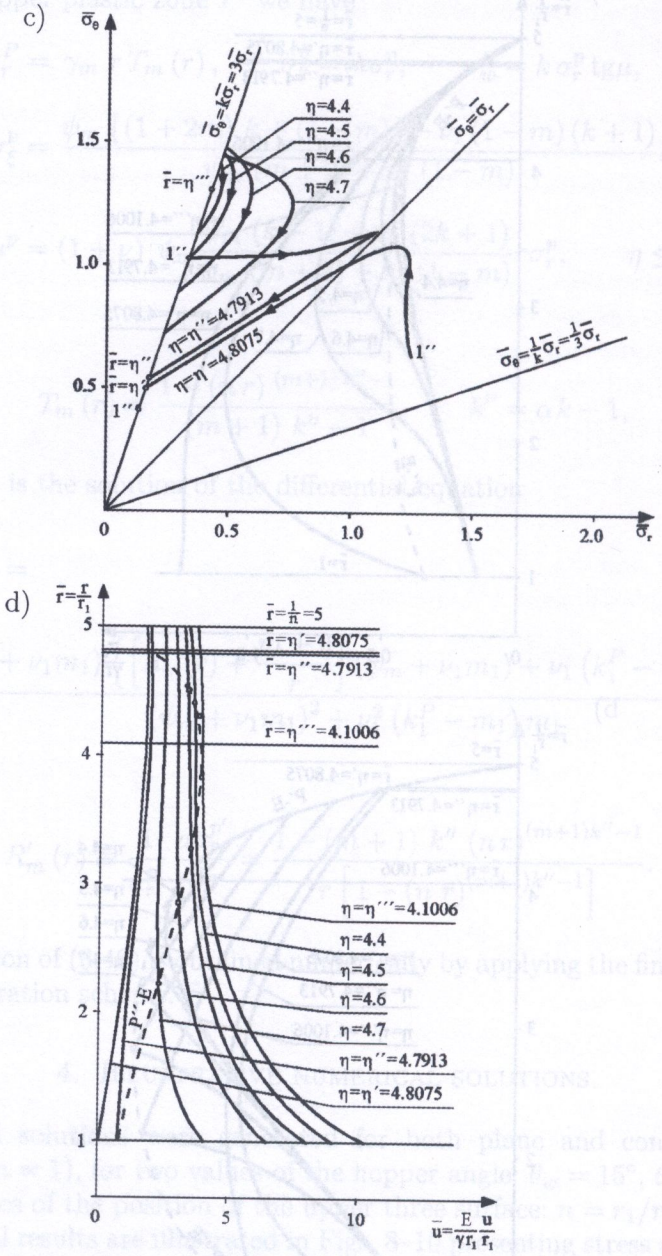

Fig. 8 Stress and displacement evolution during emptying process: a) radial stresses σ_r, b) hoop stress σ_θ, c) stress profiles, d) displacement fields; ($m = 0$, $\mu = 30°$, $\nu = 1/3$, $\theta_w = 15°$, $n = 1/5$).

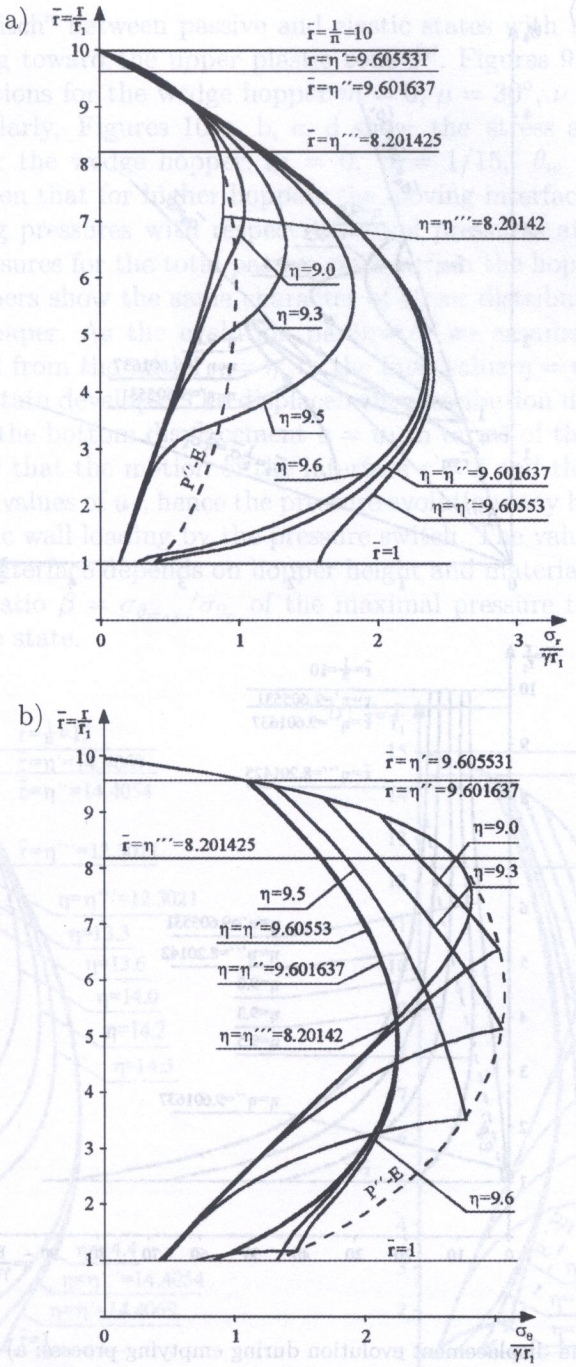
a)
$\bar{r}=\frac{r}{r_1}$
$\bar{r}=\frac{1}{n}=10$
$\bar{r}=\eta'=9.605531$
$\bar{r}=\eta''=9.601637$
$\bar{r}=\eta'''=8.201425$
$\eta=\eta'''=8.20142$
$\eta=9.0$
$\eta=9.3$
$\eta=9.5$
$\eta=9.6$
P''E
$\eta=\eta''=9.601637$
$\eta=\eta'=9.60553$
$\bar{r}=1$
$\frac{\sigma_r}{\gamma r_1}$
b)
$\bar{r}=\frac{r}{r_1}$
$\bar{r}=\eta'=9.605531$
$\bar{r}=\eta''=9.601637$
$\eta=9.0$
$\bar{r}=\eta'''=8.201425$
$\eta=9.3$
$\eta=9.5$
$\eta=\eta'=9.60553$
$\eta=\eta''=9.601637$
$\eta=\eta'''=8.20142$
P''E
$\eta=9.6$
$\bar{r}=1$
$\frac{\sigma_\theta}{\gamma r_1}$

FIG. 9. a, b

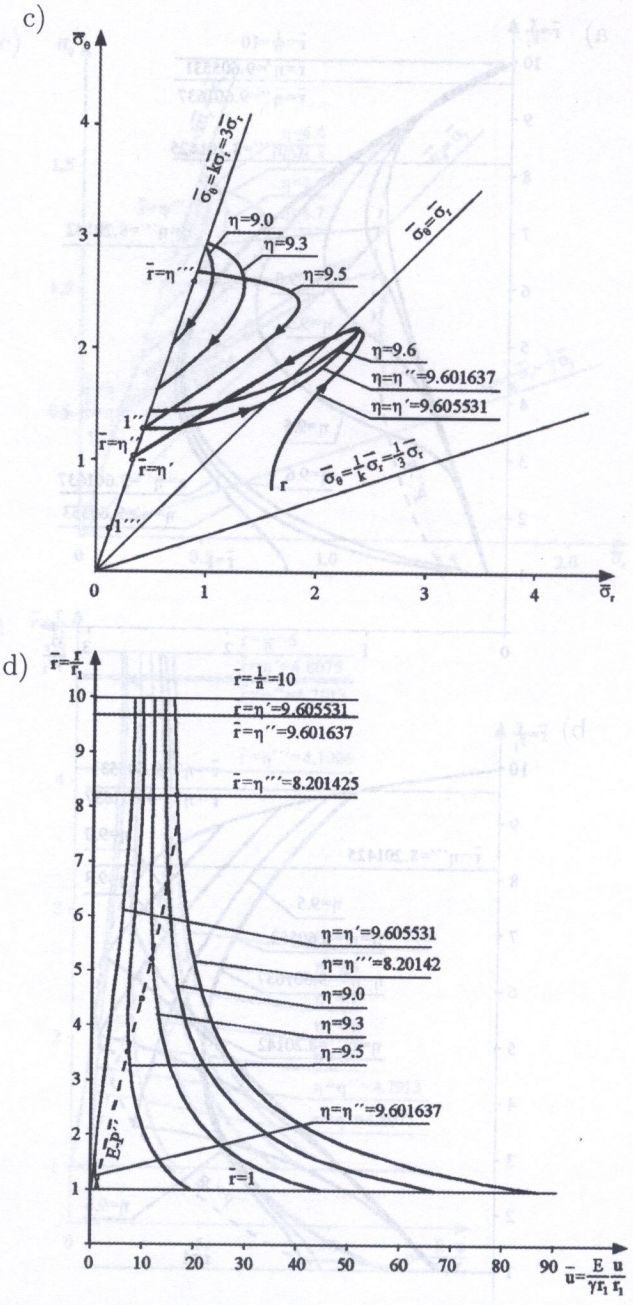

FIG. 9. Stress and displacement evolution during emptying process: a) radial stresses σ_r, b) hoop stress σ_θ, c) stress profiles, d) displacement fields; ($\theta_w = 15°$, $n = 1/10$).

is a moving "switch" between passive and elastic states with the peak pressure at $r = \xi$ moving toward the upper plastic zone P'. Figures 9a, b, c, d present similar distributions for the wedge hopper $m = 0$, $\mu = 30°$, $\nu = 1/3$, $\theta_w = 15°$, $n = 1/10$. Similarly, Figures 10 a, b, c, d show the stress and displacement distributions for the wedge hopper: $m = 0$, $n = 1/15$, $\theta_w = 15°$, $\nu = 1/3$, $\mu = 30°$. It is seen that for higher hoppers the moving interface $r = \xi$ generates higher switching pressures with respect to initial pressures at the filling stage or ultimate pressures for the total passive state within the hopper. The solution for conical hoppers show the same character of stress distributions and are not shown in this paper. As the evolution parameter we assumed the value of η which decreased from the initial $\eta = \eta'$ to the final value $\eta = \eta''$ when the total passive plastic state develops. The displacement distribution diagrams allow for specification of the bottom displacement $u = u_1$ in terms of the parameter η. It should be noted that the motion of the interface $r = \xi$ and the pressure switch occurs for small values of u_1, hence the pressure evolution may have the character of quasi-dynamic wall loading by the pressure switch. The value of overpressure due to moving interface depends on hopper height and material parameters. Let us specify the ratio $\beta = \sigma_{\theta_{\max}}/\sigma_{\theta_p}$ of the maximal pressure to the pressure at the fully passive state.

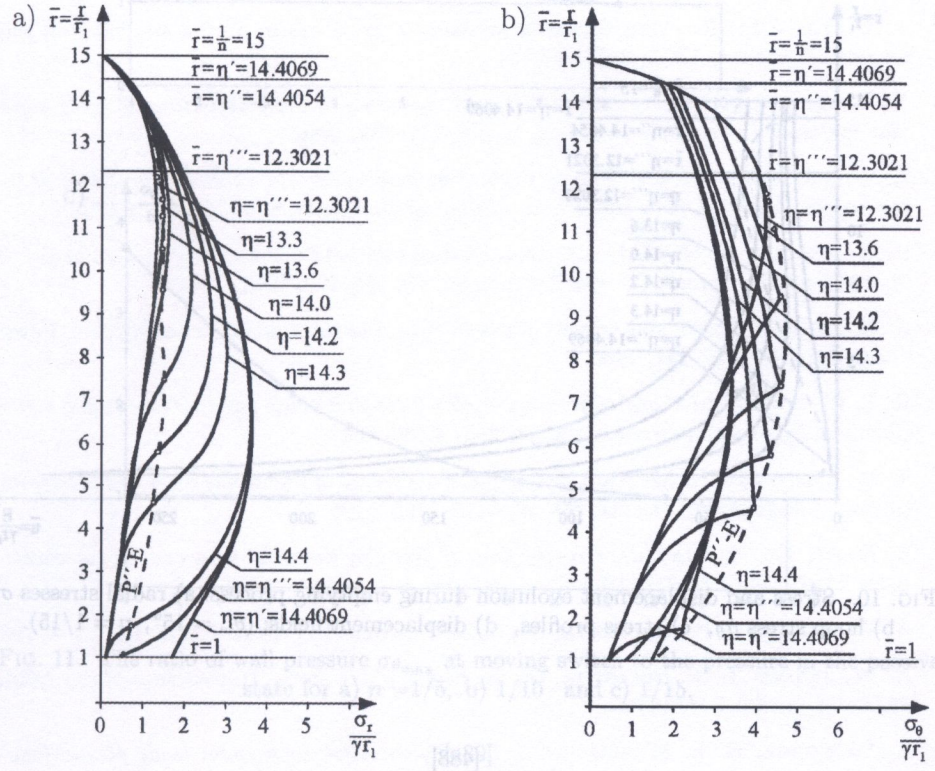

[FIG. 10 a, b]

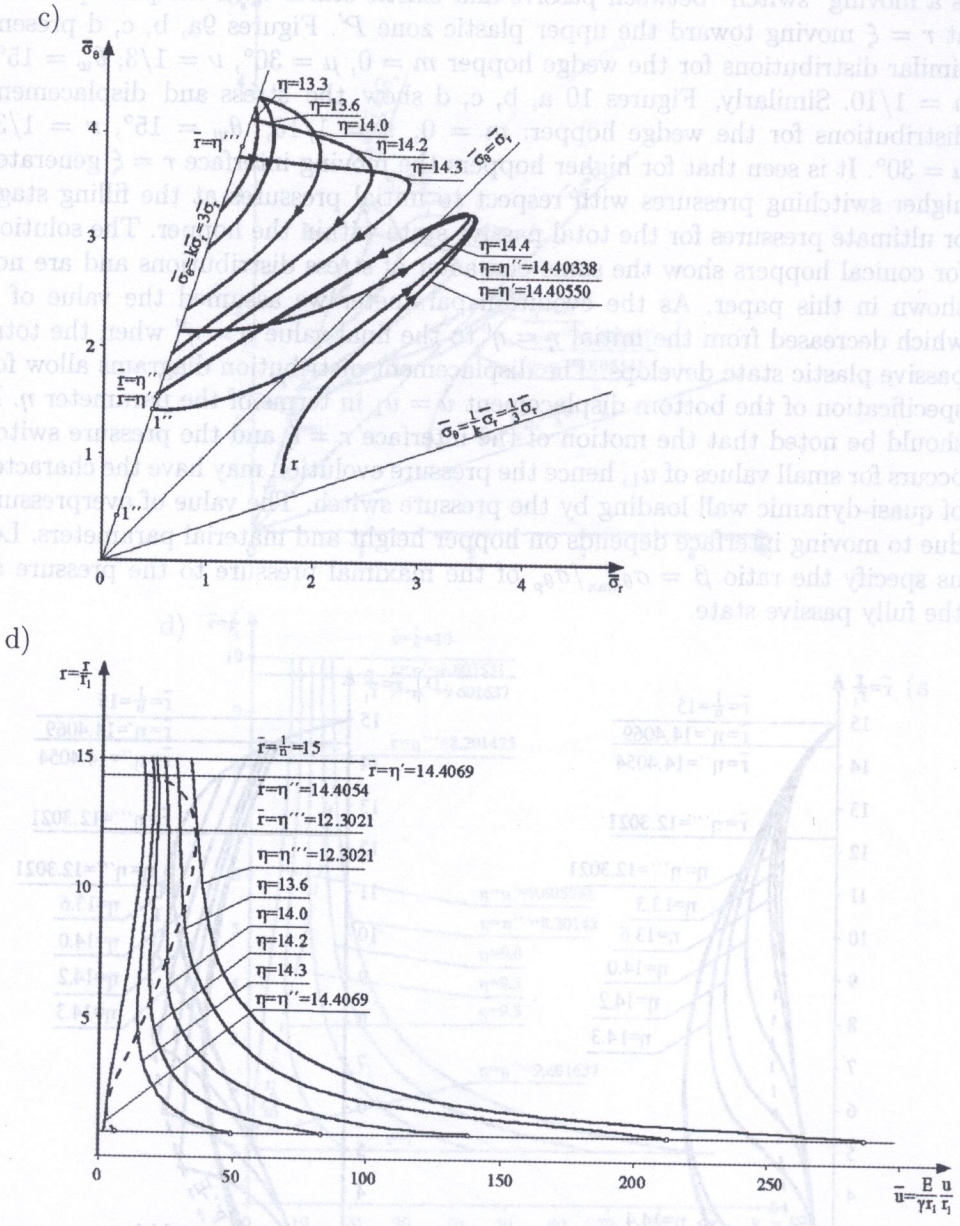

FIG. 10. Stress and displacement evolution during emptying process: a) radial stresses σ_r, b) hoop stress σ_θ, c) stress profiles, d) displacement fields; ($\theta_w = 15°$, $n = 1/15$).

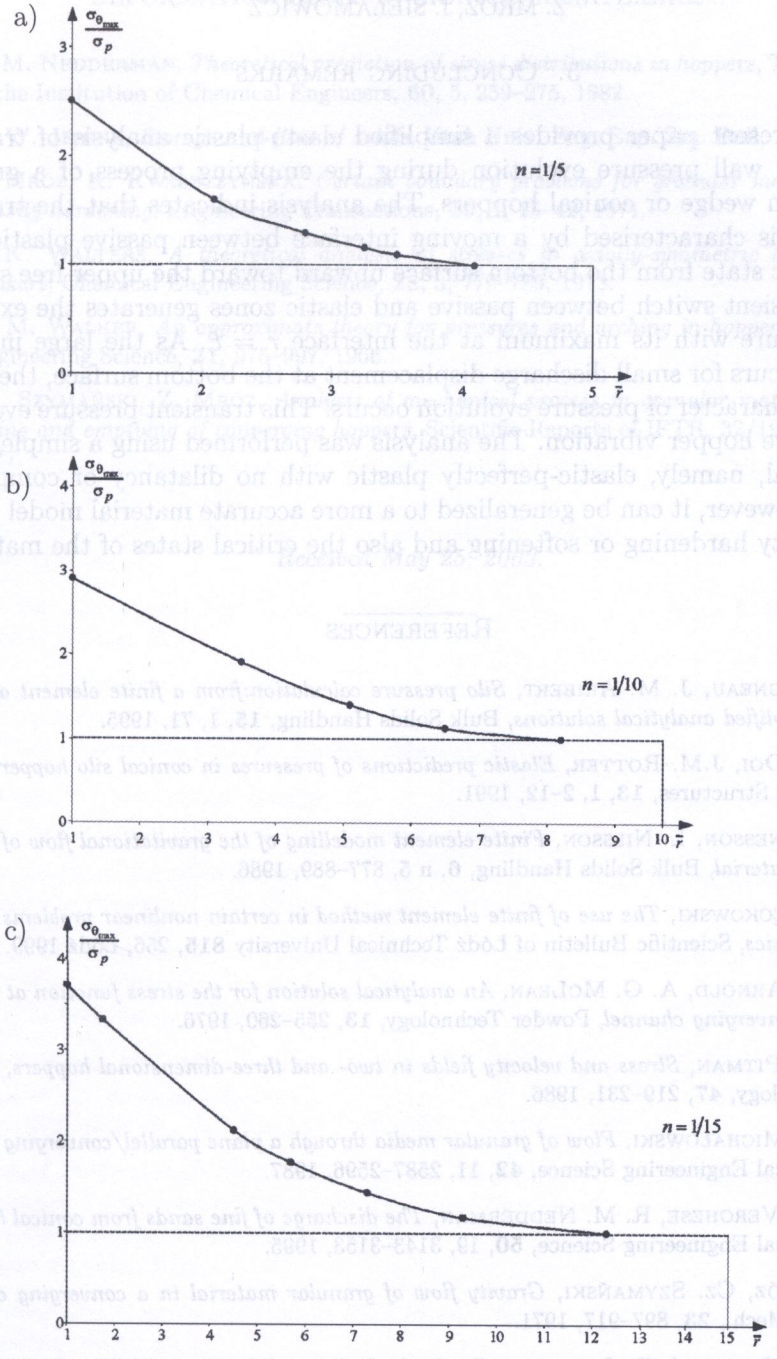

FIG. 11. The ratio of wall pressure $\sigma_{\theta_{\max}}$ at moving switch to the pressure in the passive state for a) n =1/5, b) 1/10 and c) 1/15.

5. Concluding remarks

The present paper provides a simplified elasto-plastic analysis of transient stress and wall pressure evolution during the emptying process of a granular material in wedge or conical hoppers. The analysis indicates that the transient evolution is characterised by a moving interface between passive plastic state and elastic state from the bottom surface upward toward the upper free surface. Such transient switch between passive and elastic zones generates the excessive wall pressure with its maximum at the interface $r = \xi$. As the large interface motion occurs for small discharge displacement at the bottom surface, the quasi-dynamic character of pressure evolution occurs. This transient pressure evolution may induce hopper vibration. The analysis was performed using a simple model of material, namely, elastic-perfectly plastic with no dilatancy or compaction effects. However, it can be generalized to a more accurate material model admitting density hardening or softening and also the critical states of the material.

References

1. E. Ragneau, J. M. Aribert, *Silo pressure calculation:from a finite element approach to simplified analytical solutions*, Bulk Solids Handling, **15**, 1, 71, 1995.
2. J. Y. Ooi, J.M. Rotter, *Elastic predictions of pressures in conical silo hoppers*, Engineering Structures, **13**, 1, 2–12, 1991.
3. K. Runesson, L. Nilsson, *Finite element modelling of the gravitational flow of a granular material*, Bulk Solids Handling, **6**, n 5, 877–889, 1986.
4. Z. Więckowski, *The use of finite element method in certain nonlinear problems of solid mechanics*, Scientific Bulletin of Łódź Technical University **815**, 256, Łódź 1999.
5. P. C. Arnold, A. G. McLean, *An analytical solution for the stress function at the wall of a converging channel*, Powder Technology, **13**, 255–260, 1976.
6. E. B. Pitman, *Stress and velocity fields in two- and three-dimensional hoppers*, Powder Technology, **47**, 219–231, 1986.
7. R. L. Michałowski, *Flow of granular media through a plane parallel/converging bunker*, Chemical Engineering Science, **42**, 11, 2587–2596, 1987.
8. T. M. Verghese, R. M. Nedderman, *The discharge of fine sands from conical hoppers*, Chemical Engineering Science, **50**, 19, 3143–3153, 1995.
9. Z. Mróz, Cz. Szymański, *Gravity flow of granular material in a converging channel*, Arch. Mech., **23**, 897–917, 1971.
10. A. W. Jenike, J. R. Johanson, *Bin loads*, J. Struct. Div. Proc. ASCE, **94**, ST 4, 1968.
11. A. W. Jenike, J. R. Johanson, *On the theory of bin loads*, Transactions of the ASME, **91**, Ser.B, 2, 339–344, 1969.
12. A. Drescher, R. L. Michałowski, *Density variation in pseudo-steady plastic flow of granular media*, Geotechnique, **34**, 1, 1–10, 1984.

13. R. M. NEDDERMAN, *Theoretical prediction of stress distributions in hoppers*, Transactions of the Institution of Chemical Engineers, **60**, 5, 259–275, 1982.

14. A. W. JENIKE, *Storage and flow of solids*, Utah Univ. Eng. Exp. Stn. Bull, **123**, 1964.

15. Z. MRÓZ, K. KWASZCZYŃSKA, *Certain boundary problems for granular materials with density hardening*, Engineering Transactions, **19**, 1, 15–42, 1971.

16. J. K. WALTERS, *A theoretical analysis of stresses in axially-symmetric hoppers and bunkers*, Chemical Engineering Science, **28**, 3, 779–789, 1973.

17. D. M. WALKER, *An approximate theory for pressures and arching in hoppers*, Chemical Engineering Science, **21**, 975–997, 1966.

18. CZ. SZYMAŃSKI, Z. MRÓZ, *Analysis of mechanical process in granular material during filling and emptying of converging hoppers*, Scientific Reports of IFTR, 32/1977, Warsaw 1977.

Received May 25, 2003.